JCI The Journal of Clinical Investigation

Exceptionally potent human monoclonal antibodies are effective for prophylaxis and therapy of tetanus in mice

Marco Pirazzini, … , Antonio Lanzavecchia, Cesare Montecucco

J Clin Invest. 2021. https://doi.org/10.1172/JCI151676.

Research In-Press Preview Neuroscience Therapeutics

Graphical abstract

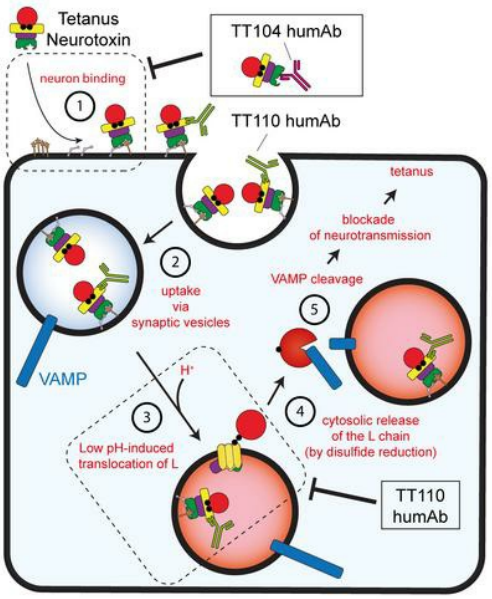

Exceptionally potent human monoclonal antibodies are effective for prophylaxis and therapy of tetanus in mice

Marco Pirazzini[1,*], Alessandro Grinzato[1,*], Davide Corti[2], Sonia Barbieri[2], Oneda Leka[1], Francesca Vallese[1], Marika Tonellato[1], Chiara Silacci-Fregni[3], Luca Piccoli[3], Eaazhisai Kandiah[4], Giampietro Schiavo[5,6], Giuseppe Zanotti[1,•], Antonio Lanzavecchia[3,7,•], Cesare Montecucco[1,8,•]

[1]Department of Biomedical Sciences, University of Padova, Via Ugo Bassi 58/B, Padova, 35131, Italy
[2]Humabs BioMed SA, 6500 Bellinzona, Switzerland
[3]Institute for Research in Biomedicine, Università della Svizzera Italiana, 6500 Bellinzona, Switzerland
[4]European Synchrotron Radiation Facility, 71 Avenue des Martyrs, F-38000 Grenoble, France
[5]Department of Neuromuscular Diseases, Queen Square Institute of Neurology, University College London, London, WC1N 3BG, UK
[6]UK Dementia Research Institute, University College London, London, WC1E 6BT UK
[7]Fondazione Istituto Nazionale Genetica Molecolare c/o Fondazione IRCCS Cà Granda Ospedale Maggiore Policlinico di Milano, Via Francesco Sforza, 35 – 20122 Milano, Italia
[8]Institute of Neuroscience, National Research Council, Via Ugo Bassi 58/B, Padova, 35131, Italy

*These authors contributed equally,

Corresponding authors:

- Prof. Giuseppe Zanotti, Department of Biomedical Sciences, University of Padova, Via Ugo Bassi 58/B, Padova, 35131, Italy, phone: +39 049 8276409, email address: giuseppe.zanotti@unipd.it
- Prof. Antonio Lanzavecchia, Istituto Nazionale Genetica Molecolare c/o Fondazione IRCCS Cà Granda Ospedale Maggiore Policlinico di Milano, Via Francesco Sforza, 35 – 20122 Milano, Italy, phone: +39 0200660300, email address: antonio.lanzavecchia@gmail.com;
- Prof. Cesare Montecucco, Institute of Neuroscience, National Research Council, Via Ugo Bassi 58/B, Padova, 35131, Italy, phone: +39 049 8276058, email address: cesare.montecucco@gmail.com

O. Leka present address: Paul Scharrer Institute, ETH Villingen, Zurich, Switzerland
F. Vallese present address: Columbia University, New York
A. Grinzato present address: European Synchrotron Radiation Facility, Grenoble, France
A. Lanzavecchia present address: Humabs BioMed SA, Bellinzona, Switzerland

ABSTRACT

Human monoclonal antibodies were used here to study the mechanism of neuron intoxication by tetanus neurotoxin and to evaluate them as a safe preventive and therapeutic substitute of hyperimmune sera for tetanus in mice. By screening memory B cells of immune donors, we selected two monoclonal antibodies specific for tetanus neurotoxin with exceptionally high neutralizing activities, which were extensively characterized both structurally and functionally. We found that these antibodies interfere with the binding and translocation of the neurotoxin into neurons by interacting with two epitopes, whose definition pinpoints crucial events in the cellular pathogenesis of tetanus. This information explains the unprecedented neutralization ability of these antibodies, which were found to be exceptionally potent in preventing experimental tetanus when injected in mice long before the neurotoxin. Moreover, their Fab derivatives neutralized tetanus neurotoxin in post-exposure experiments, suggesting their potential therapeutic use via intrathecal injection. As such, these human monoclonal antibodies, as well as their Fab derivatives, meet all requirements for being considered for prophylaxis and therapy of human tetanus and are ready for clinical trials.

Keywords: tetanus, tetanus neurotoxin, human monoclonal antibody, tetanus immunoglobulin, tetanus prophylaxis

INTRODUCTION

Tetanus neurotoxin (TeNT) is a highly potent exotoxin responsible for tetanus, a life-threatening disease whose major symptoms are muscle rigidity and spasms, spastic paralysis, respiratory deficits and autonomic dysfunctions (1-5). TeNT is produced by toxigenic strains of the anaerobic sporogenic bacterium *Clostridium tetani* (6-8). The few amino acid variations found in the currently known TeNT isoforms do not change their immunogenic properties with respect to the prototypical TeNT (Harvard strain, E88) (9).

TeNT consists of a light chain (L, 50 kDa) and a heavy chain (H, 100 kDa) linked by a single interchain disulfide bond essential for neurotoxicity (8, 10). TeNT is generally described as a protein consisting of three domains, each one serving a different step of its mechanism of neuronal intoxication. The carboxy-terminal domain HC (50 kDa) is responsible for presynaptic binding and consists of two sub-domains; the carboxy-terminal half (HC-C) contains a polysialoganglioside binding site and a nidogen binding site (11-14), whereas the amino-terminal half portion (HC-N), is essential for toxicity though its function is not known (15). HC-N is linked to HN (50 kDa), the domain responsible for the membrane translocation of the L domain into the cytosol. The L domain is a metalloprotease that blocks neurotransmitter release (16).

C. tetani spores are ubiquitous in the environment and can contaminate necrotic wounds of any kind (burns, ulcers, surgery, tattooing, circumcision and needle injection etc.) where spores may generate vegetative bacteria producing TeNT which diffuses via the blood and lymphatic circulations. TeNT binds to motor, sensory and autonomic presynaptic nerve terminals via at least two independent receptors: a polysialoganglioside and a protein (5, 17). Polysialogangliosides (PSG), including GT1b, GD1b and GQ1b, play a major role in the initial membrane binding of TeNT (11-13), whilst nidogens 1 and 2 (also known as entactin 1/2) were identified as TeNT protein receptors (14). Nidogens and PSG direct TeNT to presynaptic zones that, upon endocytosis, generate signaling endosomes containing neurotrophic factors and their receptors (18). These organelles undergo fast axonal retrograde transport to the perikaryon located in the spinal cord, where they release their content (18-20). TeNT then binds to inhibitory interneurons and is endocytosed into the lumen of synaptic vesicles (SV) (21). Acidification of the SV lumen induces a change in conformation of TeNT whereby the HN domain inserts into the membrane and assists the membrane translocation of the L chain from the SV lumen to the cytosol. Here, the interchain disulfide bond is reduced by the thioredoxin reductase-thioredoxin redox system (22), releasing the metalloprotease activity of the L domain, which specifically cleaves VAMP at a single site (23). Together with SNAP-25 and syntaxin,

VAMP forms a complex driving the fusion of SV with the presynaptic membrane with ensuing neurotransmitter release (24).

VAMP cleavage in spinal cord inhibitory interneurons prevents the release of inhibitory neurotransmitters, which determines the hyperactivation of the post-synaptic motor neurons with sustained contraction of the innervated skeletal muscles, resulting in spastic paralysis (25, 26). Muscle contractures begin with *trismus* (lockjaw, a cardinal symptom of tetanus) and neck with difficult swallowing and then descend to the thorax, causing respiratory deficit, generalized spasm of opposing skeletal muscles and autonomic dysfunctions that may lead to death (2).

Tetanus is prevented by a very effective vaccine based on tetanus toxoid that raises a long-lasting protection due to specific anti-TeNT antibodies, but after the age of forty/fifty the anti-TeNT antibody titer decreases below TeNT neutralization (27). Tetanus is still a major killer in countries where appropriate public healthcare systems are not enforced, and where the infection of the umbilical cord stump or of the birth canal with non-sterile instruments causes *tetanus neonatorum* and/or maternal tetanus (28).

Another common medical practice to prevent tetanus in patients presenting necrotic wounds at hospital emergency rooms is the injection of anti-TeNT IgG, known as tetanus immunoglobulins (TIG), isolated from hyperimmune human donors (29). Hyperimmune horse sera are used in low-income countries because of their lower cost but can generate dangerous hypersensitivity reactions. TIG is also administered to patients with symptomatic tetanus, to neutralize circulating TeNT and limit the severity of the disease though this might cause problems (see Discussion) (29). Intrathecal TIG administration is more effective, although this approach is limited by the low percentage of anti-TeNT antibodies present in TIG and by the amount of protein that can be injected in the cerebrospinal fluid (30, 31). All these drawbacks can be overcome by using highly purified human monoclonal antibodies (humAbs), which are already approved for a variety of human diseases (32-38).

Here, we report on the identification of two humAbs with extremely high TeNT neutralizing activity and determined the structure of their binding sites. These humAbs provide a long-lasting prophylactic activity against lethal doses of TeNT whereas their Fab prevented tetanus in post-exposure experiments as well as TIG. These findings suggest that these humAbs and their Fab fragments represent appropriate and safe alternatives to TIG.

RESULTS

HumAbs recognize distinct domains of TeNT and display distinct neutralizing capability.

Humabs against TeNT were isolated from memory B cells of immune adult donors who underwent booster vaccinations with tetanus toxoid as described (33). IgG memory B cells were immortalized under clonal conditions and the antibodies produced in the culture supernatant were screened by ELISA for their ability to bind TeNT. The antibody genes from 14 positive clonal cultures were sequenced and recombinant antibodies were produced as IgG1 by transfecting HEK-293 cells.

The TeNT domains recognized by the 14 humAbs were determined by western blotting of the intact or reduced toxin and of the recombinant sub-domains (Figure 1). The binding specificity of each antibody is shown in Figure S1. 11 antibodies bound to the HC domain, 3 to the HN domain and none to the L chain. 3 out of the 11 HC-specific antibodies recognized the HC-C part, 8 of them bound to the HC-N portion (Figure S1), suggesting that HC-N is the most immunogenic part of TeNT. Recent studies on anti-TeNT humAbs reported that the highest TeNT neutralization was displayed by antibodies recognizing HC, particularly those preventing PSG binding, but did not report on HC-N recognition (39-42). Although the role of HC-N in neuron intoxication is currently unknown, its deletion causes loss of toxicity (15). Therefore, these specific humAbs could be very useful in unravelling the role of HC-N in the molecular and cellular pathogenesis of tetanus. Together with the knowledge that HC-C contains the binding sites for the neuronal receptors of TeNT, these findings strongly suggest that the structure of TeNT is best described in terms of four domains (L, HN, HC-N and HC-C), rather than the three-domain paradigm (L, HN and HC) reported so far (8, 43).

Inhibition of TeNT activity by humAbs.

HumAbs were tested in cerebellar granule neurons (CGNs) for their ability to inhibit TeNT cleavage of VAMP-2, an isoform highly expressed in central nervous system neurons. CGNs were chosen because they are highly susceptible to TeNT, and VAMP cleavage is easily testable by immunoblotting and imaging (44). Figure 2A shows that an overnight incubation of CGNs with 50 pM TeNT is sufficient to cleave all the VAMP-2 of these neurons. An initial screening with a hundred-fold molar excess showed that only 4 out of the 14 humAbs tested (TT104, TT110, TT109 and TT39) were able to prevent TeNT action, albeit to different extents. Accordingly, we focused on these humAbs and tested various humAb:TeNT molar ratios to determine their neutralizing potency. As shown in Figure 2B, TT39 and TT109 showed partial neutralization. In contrast, both TT104 and

TT110 prevented TeNT intoxication already at a low molar ratio, TT104 being the most powerful. These results were paralleled by immunofluorescence staining of VAMP-2 (Figure 2C).

The selected humAbs were then tested for their ability of neutralizing TeNT *in vivo*. Figure 2D shows that preincubation of TeNT with TT104 and TT110 prevented the development of tetanus in mice in a dose-dependent manner, with TT104 displaying full neutralization at equimolar ratio. On a molar basis, TT110 was less effective, but reduced tetanus symptoms at a 2.5:1 molar ratio and completely neutralized TeNT at a 5:1 ratio. TT39 and TT109 did not protect mice from TeNT challenge. Accordingly, TT104 and TT110 were chosen for further structural and functional analyses.

Structure of the ternary complex of TeNT with TT104 and TT110 Fab.

Recombinant Fab fragments of TT104 and TT110 were produced by introducing a stop codon after C_H1 domain (Figure S2). The dissociation constants of the toxin-Fab complexes were measured by surface plasmon resonance using immobilized TeNT as a bait and found to be 6.7×10^{-12} M and 3.0×10^{-9} M for TT104-Fab and for TT110-Fab, respectively (Figure S3). The high affinity of these interactions suggested the possibility that stable binary and ternary complexes could be formed between TeNT and the two Fab. Indeed, immunocomplexes were obtained by incubation of single components either in binary (1:1) or in ternary mixtures (1:1:1) (Figure S4). The ternary [TeNT]-[TT104-Fab]-[TT110-Fab] immunocomplex was purified to homogeneity by gel filtration (total mass 250 kDa). Attempts to crystallize this complex were not successful and therefore we switched to cryo-EM that produced a model fitting the available structure of TeNT (PDB ID 5n0b) and of the two Fabs modelled using the sequences of TT104 and TT110 Fabs. The overall four-domain folding of TeNT is well conserved in the immunocomplex and superimposes with the structures of isolated domains (Figure 3A and 3B) and of the whole toxin (Figure 3C and 3D) (8, 45-47).

Similarly to TeNT alone (8), the trimeric complex [TeNT]-[TT104-Fab]-[TT110-Fab] in solution is flexible (Figure S5A). The flexibility is intrinsic to TeNT and not influenced by the binding of the Fabs; it is mainly located around residues 870-875, a loop not resolved in the crystal structure of the toxin and corresponding to the connection between the C-terminal of HN and the N-terminal of HC-N (8). To overcome the flexibility of the complex, the structure was split in two parts analyzed separately and two masks were generated by the multi-body technique to yield two different maps, one relative to [TeNT-L-HN]-[TT110-Fab], and the other one to [TeNT-HC]-[TT104-Fab].

Structure of [TeNT-L-HN]-[TT110-Fab].

Owing to the preferred orientation assumed by the particles in the grid, the analysis of [TeNT-L-HN]-[TT110-Fab] portion provided a resolution of 8.3 Å, insufficient to define their interactions at the atomic level. However, the overall shapes could be clearly distinguished and showed that TT110-Fab binds the HN domain opposite to the L domain (Figure 3A). The buried surface of this epitope was estimated to be 700 $Å^2$ and 380 $Å^2$ for chains V_H and V_L, respectively, and the interaction area involves the TeNT helices 597-607 and 614-625, extending to the following strand until residue 631 and including segment 655-663. Importantly, this latter segment is part of the "BoNT-switch", a structural module proposed to be a main driver of the low-pH induced membrane insertion of HN in the botulinum neurotoxins (BoNT), a group of toxins sharing the structural architecture and the mechanism of neuron intoxication of TeNT (49). The BoNT-switch is composed of disordered loops and three short helices (α_A, α_B, α_C) that are also present in TeNT (Figure S7); TT110-Fab binds to a region in TeNT corresponding to the α_B of BoNT serotype A1 (BoNT/A1) (Figure S8). At acidic pH, the BoNT/A1-switch rearranges into five β strands (dubbed β1–β5) with α_A flipping out from the toxin structure at the center of an elongated hinge formed by β2/β3 hairpins (corresponding to residues I630–Y648 in BoNT/A1 and to V639-Y657 in TeNT). This hinge was shown to insert into the lipid bilayer and to be essential for the subsequent membrane translocation of the L domain of BoNT/A1 (49). At the same time, α_B and α_C form the β4/β5 hairpin with a hydrophobic surface generated by the structural rearrangement. Considering that TT110-Fab binds to α_B, it is very likely that it neutralizes TeNT by interfering with the low pH driven insertion of HN into the membrane, thus blocking the translocation of the L domain into the cytosol.

Structure of [TeNT-HC]-[TT104-Fab].

The map of the portion of the complex including TT104-Fab and the HC-N and HC-C domains (residues 875-1110 and 1111-1315, respectively) has an overall resolution of 3.9 Å. The area of interaction of the antibody with the HC-C domain is opposite to the HN and L domains and includes portions of polypeptide strands 1140-1145, 1149-1157, 1171-1173, 1202-1204 and 1276-1281 (Figure 3B). From the Fab side, the interaction involves mainly the V_H chain whose surface area buried upon the binding is 555 $Å^2$, whilst the buried area of chain V_L is 396 $Å^2$. This difference is reflected in the number of interactions. V_H residues form one salt bridge and seven potential hydrogen-bonds, whilst V_L contributes to stabilize the protein-protein interaction with additional four hydrogen bonds (Supplementary Table 1, calculation performed with server PISA) (48). The total TeNT buried surface in the complex with TT104-Fab is 792 $Å^2$.

The TT104-Fab binding site is only 12 Å away from the putative nidogen binding site modelled previously (14) and its proximity suggests a possible interference with the binding of nidogen to HC-C due to a steric clash (Figure S6). At the same time, this binding might alter the ability of HC-C to interact with the oligosaccharide portion of PSG, which projects out the neuronal plasma membrane and has to be accommodated into the HC-C to mediate binding (17). These possibilities have been tested experimentally (see below).

Model of the overall structure of the immunocomplex*.*

Owing to the intrinsic flexibility of the complex in solution, it was not possible to obtain a complete 3D map of the entire immunocomplex. Nevertheless, thanks to the available crystal structure of TeNT (8, 39), we built a model of the ternary complex by superimposing the L, HN, HC-N and HC-C domains to the TeNT crystal structure (Figure 3C). The flexibility of the TeNT-Fabs complex observed in our images is intrinsic to TeNT (8) and, accordingly, this model represents one of the possible conformations of the toxin with the two Fabs bound. We detected several eigenvalues (Figure S5B and C) that define the dynamics of the motion of the L-HN domains relative to the HC-N and HC-C domains. All the eigenvalues are unimodal, suggesting that these motions are continuous. The first three eigenvalues describe 85% of the variability present in the dataset. The movies of the reconstructed body repositioned along these eigenvectors reveals that the two domains of TeNT have a rocking motion (Supplementary movies 1, 2 and 3). Interestingly, the conformation of TeNT in the immunocomplex is closer to the open conformation of the full-length toxin in which the C869-C1093 disulphide bond was reduced (39) than to that of the non-reduced TeNT (8).

TT104-Fab inhibits the biological activity of TeNT by preventing membrane binding.

TT104-Fab prevents cleavage of VAMP in CGNs and the development of tetanus in mice (Figure 5A and B). The TeNT-TT104-Fab interaction suggests that this Fab should interfere with toxin binding. As detected using a fluorescently labelled HC fragment (A555-TeNT-HC, red signal in Figure 5C and D), TT104-Fab prevents the binding of TeNT both to CGNs and to the neuromuscular junction (NMJ). TT104-Fab inhibition is very specific, as indicated by the lack of interference with the binding of a fluorescent HC of BoNT/A1 (CpV-BoNT/A1-HC, green signal in Figure 5C and D). Of note, the signal of CpV-BoNT/A1-HC is slightly brighter in the presence of TT104-Fab, which sequesters A555-TeNT-HC preventing the competition of the two toxin HCs for PSG binding (green signals in Figure 5C and D).

To elucidate the specific mechanism responsible for the TT104-Fab-mediated inhibition of TeNT binding, we assayed the interaction of TeNT with immobilized GT1b, purified nidogen-1 and -2, or their combinations. Figure 5E shows that TeNT binding to GT1b is completely prevented by TT104-Fab, whilst binding to nidogens is strongly reduced. This result is in line with the definition of the surface of the conformational epitope recognized by the idiotype of TT104-Fab. Interestingly, when GT1b and nidogens are immobilized together (Figure 5E, right panel), TeNT binding in the presence of TT104-Fab compares to that reached when only nidogens are present. These findings support the model of nidogen-TeNT interaction occurring at a distinct site with respect to that of PSG (14), and indicate that TT104-Fab interferes with the binding of both receptors. At the same time, these results clearly indicate that membrane binding is the specific step inhibited by TT104 and TT104-Fab, with a consequent strong anti-tetanus activity *in vivo*.

TT110-Fab inhibits the low pH induced conformational change of TeNT.

Although less powerful than TT104-Fab, also the HN-specific TT110-Fab effectively prevents the cleavage of VAMP by TeNT in cultured neurons (Figure 6A) and protects mice from a TeNT challenge when the toxin and the Fab are pre-incubated together before i.p. injection (Figure 6B). As discussed before, the structure of the immunocomplex suggests that TT110 interferes with the HN-dependent membrane translocation of the L chain driven by acidification. After neurotransmitter release, SV are endocytosed and acidified by the vacuolar ATPase, a process necessary for neurotransmitter re-loading. TeNT inside SV in central neurons (21) exploits this physiological process to change structure with exposure of hydrophobic patches on HN that mediate its membrane insertion in such a way as to assist the membrane translocation of the L domain (50). As this process cannot be experimentally accessed from the outside of the cells, we took advantage of a method previously devised to induce the low pH membrane translocation of the L chain directly from the plasma membrane into the cytosol (50-53). As schematized in Figure 6C, after TeNT binding to neurons at 0^{o} C, membrane translocation is induced by replacing the cold medium with acidic medium at 37°C for few minutes. Neurons are then incubated in control medium in the presence of bafilomycin A1, a v-ATPase inhibitor preventing toxin entry through the canonical route, and L domain translocation is assessed by determining VAMP-2 cleavage. Figure 6D shows that upon exposure to pH 5, the L metalloprotease enters the cytosol and efficiently cleaves VAMP-2. In contrast, when TeNT is pre-incubated with TT110-Fab, VAMP-2 is no longer cleaved, consistent with a block of translocation.

To test the possibility that TT110-Fab prevents the low pH-induced structural change of TeNT (51, 54, 55), we performed a fluorometric assay based on the binding of the lipophilic dye ANS to hydrophobic protein patches (56). Figure 6E shows that TT110-Fab prevents TeNT from undergoing the low pH-driven conformational change with exposure of hydrophobic surface patches. This result supports the hypothesis that TT110 blocks the "BoNT/TeNT-switch" of HN and prevents the occurrence of the low pH-driven insertion of HN and the following membrane translocation of the L domain. Considering these results and the available literature, we propose that the protonation of Asp618, Asp621, Asp622, Glu626, Glu658, Glu666 of TeNT (Figure S8), is likely to be the key initial event of the low pH conformational transition of HN leading to its membrane insertion. Future mutagenesis experiments targeting these residues will provide conclusive evidence on the role of these acidic sites in the molecular pathogenesis of tetanus.

Collectively, the above experiments demonstrate that TT110-Fab and TT104-Fab act on two different steps of the process of TeNT nerve terminal intoxication, predicting that they should display additive effects in preventing experimental tetanus *in vivo*.

Prophylaxis and therapy of experimental tetanus by TT104, TT110 and their Fabs.

The most frequently used protocol of testing the neutralizing activity of anti-TeNT antibodies involves their pre-incubation with TeNT. This procedure does not match the conditions of injured patients where IgG anti-TeNT are used as tetanus prophylactic agents before the toxin is produced by *C. tetani* in necrotic wounds. Therefore, we performed a set of experiments in which mice were pre-treated with a single intraperitoneal injection of TT104 and TT110, alone or in combination, before inoculating 5 MLD_{50} of TeNT at delayed time points. Since tetanus usually develops with incubation times ranging between 2 and 15 days after injury (1, 2), animals were pretreated with the TT104 and TT110 alone (400 ng/kg each) or in combination (200 ng/kg+200 ng/kg) 7 and 15 days before TeNT injection (Figure 7A). As a control, we pretreated a cohort of animals with TIG (7 IU/kg, corresponding to the standard prophylaxis with 500 IU used in a human of 70 kg). Remarkably, TT104 provided full protection of mice from tetanus, even when injected 15 days before TeNT (Figure 7B). TT110 was less effective since it was fully protective only when challenge was performed on day 7 (Figure 7C). The combination of 200 ng/kg of TT104 and of 200 ng/kg of TT110 provided a full protection of mice for 15 days, as TIG did (Figure 7D).

Once the metalloprotease domain of TeNT has been released inside the cytoplasm of target neurons, the toxin cannot be neutralized any longer by anti-TeNT antibodies. However, worsening

of the symptoms can be prevented by neutralization of circulating TeNT, and this is the reason supporting the general practice of injecting TIG into hospitalized patients showing symptomatic tetanus. Thus, TIG and TT104 or TT110 were compared in a therapeutic setting for their capacity to interfere with tetanus at different time points after TeNT challenge. We opted to use the Fab derivatives in consideration of their possible use by intrathecal rather than peripheral administration. To properly compare the Fabs and TIG, we estimated the concentration of anti-tetanus specific IgG present in the standard dose of 500 IU (in a putative patient of 70 kg) based on previous quantifications on the serum of hyper-immunized human donors (57). As shown in Figure 7E, TeNT inoculation (4 ng/kg) was followed by injection of either TIG or the corresponding amount of TT104-Fab and TT110-Fab in combination after different time periods (1.5, 3, 6 and 12 hours). Table 1 shows that the Fab combination completely protected mice, as TIG did, up to 6 hours after injection of TeNT. However, both forms of serotherapy did not block the toxin completely when injected 12 h after TeNT challenge, in agreement with what is known on the kinetics of TeNT internalization into neurons (5). Notably, in this case, mice developed tetanus symptoms with a similar time course (Figure 7F), further indicating that the Fab combination and TIG are comparably effective in neutralizing the activity of the toxin present in body fluids.

DISCUSSION

Here we report the structural and functional characterization of two human monoclonal antibodies that prevent tetanus by neutralizing TeNT at nearly stoichiometric antibody:toxin ratios, a property maintained by their Fabs. TT104 interacts strongly with the HC-C domain that mediates TeNT binding to neurons, whilst TT110 binds the HN domain that mediates the translocation of the metalloprotease domain into the neuronal cytosol.

The structure of the [TeNT]-[TT104-Fab]-[TT110-Fab] trimeric immunocomplex has been resolved by cryo-EM and the two TeNT epitopes were identified. This information explains why these antibodies are so potent in preventing tetanus in mice, also after being administered up to 15 days before TeNT. These results are even more relevant considering that the lifetime of human IgGs in mice is expected to be lower than that in humans (58, 59), leading to the prediction that the duration of the great protection exerted by TT104 and TT110 will be even longer in humans. In addition, it should be considered that these antibodies could be engineered to achieve extended half-life and bio-distribution (60). Remarkably, TeNT neutralization was effective in the ng/kg range, a dose

orders of magnitude lower than the mg/kg range of TIG, offering the possibility of increasing the dose, if necessary.

To the best of our knowledge, this is the first report showing such a potent and long-lasting prophylactic effectiveness of anti-TeNT human monoclonal antibodies, which fully meets the needs of patients entering hospital emergency rooms with necrotic wound(s) possibly contaminated by *C. tetani* spores. TT104 and TT110 are expected to be very effective also in preventing maternal and/or neonatal tetanus in the case of delivery from a mother not immunized against tetanus, a frequent condition in several parts of the world (28).

The current serotherapy with IgG isolated from the blood of hyperimmune donors, is affected by a number of drawbacks: i) variation of neutralizing power from lot to lot; ii) possible risk of contamination with unknown viruses or with blood proteins, iii) need of injecting relatively large amounts of proteins (typically 16 – 20 % w/v), which may elicit adverse reactions such as angioedema or anaphylaxis, iv) high risk of anaphylactic reactions or serum sickness in the case of horse antisera, v) in addition, patients with IgA deficit could mount an immune response to the small amount of IgA present in TIG. Pain at the site of injection or fever, dizziness and other side effects are not uncommon. All these problems could be overcome by the injection of small amounts of well characterized monoclonal antibodies, such as those identified in this study, or even a single one as exemplified by TT104. Our findings also pave the way to the use of Fab fragments via the intrathecal route. This procedure was found to provide better results than peripheral injections when the toxin has already undergone retroaxonal transport and has been released into the spinal cord but is strictly limited by the amount of antibody protein that can be safely injected intrathecally (30, 31).

The isolation of anti-TeNT humAbs from human B memory cells was recently reported (39-42). TeNT neutralization in mice could be achieved only by preincubation of the toxin with a combination of 3 antibodies and/or using high molar excess of humAbs with respect to TeNT. As in the present study, the highest neutralizing effect was provided by antibodies specific for the HC binding domain of TeNT. This notion agrees with the numerous reports about the activity of monoclonal antibodies specific for the HC portion of TeNT isolated from mice, or prepared after humanization procedures, or by scFv antibody phage display library (61, 62). Together with our findings with TT104, these data fit with the rather general rule that neutralizing antibodies interfere with pathogen binding to its receptor. However, it is interesting to note that the strong neutralizing activity of TT110 indicates that antibodies can also effectively neutralize TeNT by blocking its membrane translocation.

Nine humAbs identified in the present study recognize the HC-N domain, 3 humAbs bind the HC-C domain and 3 bind the HN domain. These results suggest that the most immunogenic domain of TeNT is HC-N, but this possibility calls for more extensive studies. In addition, the fact that HC-N specific humAbs have negligible neutralization activity suggests a structural role for the HC-N domain. This interpretation is in line with the result of Masuyer et al., who showed a direct interaction at low pH of the L and HC-C domains, but not with the HC-N (8).

In addition to the biomedical properties of the two anti-TeNT humAbs, the structure of the immunocomplex formed by the toxin with the two Fab derivatives brought novel information on two key steps of the mechanism of nerve terminal intoxication by TeNT. The first insight is about the sequential events leading to a productive binding of TeNT to the presynaptic membrane at the NMJ. TeNT binds both a PSG molecule and the protein nidogen-1/2, but the sequence of binding events is not known. Nidogens are particularly enriched in the NMJ basal lamina which enwraps perisynaptic Schwann cells and the nerve terminal secluding them from the muscle fiber. Nidogens are in a strategic position to capture TeNT molecules entering the NMJ, because they are exposed to the perineural extracellular fluids, yet they are engaged in multiple protein-protein interactions with other basal lamina components, which may limit their availability for TeNT fixation. PSG are glycolipids located on the outer leaflet of the presynaptic membrane, which are endowed with long and flexible headgroups projecting above the plasma membrane. Our data show that TT104 fully disrupts TeNT interaction with PSG but only partially with nidogens, yet this is sufficient to abrogate TeNT binding and internalization at nerve terminals and to prevent tetanus. This strongly suggests that the interaction with PSG is a prerequisite for TeNT toxicity and it is the first step of TeNT binding. Nidogens might then drive the TeNT-PSG complex towards the specific endocytic organelle leading to the formation of signaling endosomes (63).

Experiments with TT110 provided new insights on the mechanism of TeNT entry into nerve terminals. TT110-Fab was found to prevent the low pH-driven conformational change of HN by binding to an epitope at the center of an important structural-functional module, the BoNT-switch, previously identified in BoNT/A1, which was suggested to be the pH sensor triggering the initial event of HN membrane insertion (49). The present work indicates that such a structural switch also occurs in TeNT. In addition, the TeNT epitope recognized by TT110 identifies a group of carboxylate residues that are candidates for future studies aimed at determining their role in the TeNT low pH-triggered switch for membrane insertion.

The results described here qualify the humAbs TT104, TT110 and their Fabs derivatives as novel therapeutics highly superior to the presently used anti-tetanus immunoglobulins. These humAbs are ready, after appropriate formulation, to replace the immunoglobulins purified from human or equine blood in clinical practice. Their Fab derivatives open new avenues to the treatment of tetanus patients because large doses could be injected intrathecally, thus maximizing the ability of these novel therapeutics to neutralize TeNT in the very area of its action, i.e. the spinal cord.

METHODS

Human monoclonal antibodies and Fab fragments

30-50 x 10^6 peripheral blood mononuclear cells (PBMCs) were isolated from adult donors who had received a boost dose of tetanus toxoid vaccine at least one year before sampling. Memory B cells were isolated from PMBCs using magnetic cell sorting with 0.5 µg/ml anti-CD19-PECy7 antibodies (BD, 341113) and mouse anti-PE microbeads (Miltenyi Biotec, 130-048-081) followed by FACS sorting using 3.75 µg/ml Alexa Fluor 647–conjugated goat anti-human IgG (Jackson ImmunoResearch, 109-606-170), 5 µg/ml Alexa Fluor 647–conjugated goat anti-human IgM (Invitrogen, A21215) and PE–labeled anti-human IgD (used at 1:40 dilution; BD Biosciences, 555779). Sorted B cells were immortalized with Epstein–Barr virus (EBV) and plated in single-cell cultures in the presence of CpG-DNA (2.5 µg/ml) and irradiated PBMC-feeder cells, as previously described (35). Two weeks post-immortalization, the culture supernatants were tested (at a 2:5 dilution) for binding to TeNT by ELISA. Briefly, ELISA plates were coated with 1 µg/ml of TeNT. Plates were blocked with 1% BSA and incubated with titrated antibodies, followed by 1/500 alkaline phosphatase (AP)-conjugated goat anti–human IgG (Southern Biotech, 2040-04). Plates were then washed, substrate (para-nitrophenyl phosphate (p-NPP, Sigma) was added and plates were read at 405 nm.

Recombinant Fab fragments were produced in HEK-293 cells by introducing a stop codon at the end of C_H1 and purified by affinity chromatography on AKTA Xpress Mab System (Cytiva) with UNICORN 5.11 software version (Build 407) using CaptureSelect C_H1-XL MiniChrom columns (ThermoFisher Scientific), buffer exchanged to PBS using a HiPrep 26/10 desalting columns (Cytiva). Purified Fabs were concentrated by Amicon Ultra filter units (Millipore), sterilized through a 0.22 mm filter and stored at -80°C after rapid freezing in liquid N2.

Cryo-EM data collection and processing

A first screening of the sample and its analysis with Cryo-EF (64) suggested a strong particle's orientation (data not shown). To overcome this problem, data were acquired on a planar orientation and 30° tilted one. For the planar acquisition, 3 ml of the sample at 0.5 mg/ml concentration, were applied to glow-discharged C-flat 2/1 -3 Au holey grid and vitrified in a Mark IV Vitrobot (FEI), whereas, for the tilted acquisition, 3 μl of the sample at 0.35 mg/ml concentration were applied to glow-discharged Aultrafoil 1.2/1.3 grid. Both grids were imaged in a Titan Krios microscope (Thermo Fisher Scientific) at 300 keV with a K2 direct electron camera at 0.827 Å per pixel. The planar dataset is composed by 402 movies (40 frames each and a dose of 1.2 $e^-/Å^2$) and was combined with the tilted dataset containing 2970 movies (50 frames each with 0.68 $e^-/Å^2$) after beam-induced motion correction with Motioncor2 (65) and Contrast transfer function (CTF) estimated with Gctf (66). The selected micrographs were picked and analyzed in RELION-3 (67). An initial model generated with EMAN2 (68) was used for the 3D classification and refinement. An analysis of the 2D classes and of the obtained 3D model suggests the presence of some mobility of the domains of the toxin. To overcome this problem, a multibody refinement procedure was performed (69). This refinement gives twelve motion eigenvalues with the first three that explain the 85% of the variance in the data. These eigenvalues allow one to align and subtract the signal of the two domains of the protein and to perform a local reconstruction of the two main flexible regions (70, 71) (see workflow in Figure S5). This protocol yielded a 3.9 Å resolution map that matches to the density of the HC domain and the TT104-Fab formed by 98170 particles, and a 8 Å low-resolution map of the LC-HN domains bound to TT110-Fab.

HumAbs subdomain specificity

TeNT (0.5 μg), reduced TeNT (0.5 μg in 15 mM of dithiothreitol), TeNT-HC (1 μg) or the individual subdomains (HC-C and HC-N) were separated by SDS-PAGE and transferred on nitrocellulose membranes. After saturating for 1 hour with 5% BSA in PBS containing 0.5% of Tween (PBS-T), membranes were incubated (overnight at 4°C) with HumAbs diluted in PBS-T (1 ug/ml) used as primary antibodies. After washing, membranes were incubated with anti-human secondary antibodies conjugated to HRP for 1 hour and then revealed with an Uvitec gel documentation system (Cleaver Scientific) using Luminata Crescendo (Millipore) as substrate.

TeNT neutralization assay on primary neuronal cultures

Primary CGNs were prepared from 4- to 6-day-old rats as previously described (44). CGNs at 6–8 days in vitro (DIV) were treated with TeNT (50 pM) alone or pre-incubated for 1 hour at RT at the indicated molar ratios of TeNT:humAbs or TeNT:Fabs in complete BME. After 12 hours, CGNs were lysed with Laemmli sample buffer containing protease inhibitors (Roche) or fixed for 10 min with 4% (w/v) paraformaldehyde in PBS. Neutralization was determined by western blotting monitoring the cleavage of intact VAMP-2 (Synaptic System, 104 211) and SNAP-25 (Biolegend, SMI81) as loading control (44).

Fixed CGNs were analyzed by immunofluorescence staining with primary antibodies specific for intact VAMP-2 (Synaptic System 104 211) detected with a fluorescent secondary antibody (44). DAPI stained the nuclei. Coverslips were mounted using Fluorescent Mounting Medium (Dako) and examined with a Leica SP5 confocal microscope (Wetzlar, Germany).

Internalization of fluorescent HC derivatives.

BoNT/A-HC-CpV (50 nM) and TeNT-HC-555 (50 nM) were mixed for 1 hour at 37°C in complete BME with or without TT104-Fab (30 nM), and then added onto CGNs 6-8 DIV seeded on glass coverslips. At indicated time points, cells were gently rinsed with medium and incubation stopped with 4% paraformaldehyde. Coverslips were extensively washed, mounted and fluorescence examined with a Leica SP5 confocal microscope.

In mice, 1 µg of TeNT-HC-555 and BoNT-HC-CpV were mixed in “bioassay solution” (0.9 % NaCl, 0.2 % gelatin). Then the solution was split and incubated for 1 hour at 37°C with either TT104-Fab (5 molar excess) or the corresponding volume of bioassay solution. 20 µl of either mixtures were injected below the skin at the level of the *Levator Auris Longus* (LAL) of anesthetized CD1 mice. After 2 hours, the LALs were dissected, fixed with 4% paraformaldehyde and directly mounted in mounting medium for microscopy analysis with a Leica SP5 confocal microscope.

Binding assay to polysialoganglioside GT1b and nidogens

96-well-plates (Sarstedt, Germany) were coated with either 1 µg of GT1b (Santa Cruz Biotechnology, USA) dissolved in methanol, or 250 ng of nidogen-1/2 (Bio-Techne, USA) diluted in PBS, or their combinations and let to dry overnight at room temperature. Wells were washed with PBS-T, blocked with 1% BSA in PBS for 1 h at RT, and the indicated concentrations of TeNT diluted in PBS, with or without pre-incubation with TT104-Fab (1 hour at RT) were added for 2 hours at RT. Wells were then extensively washed with PBS-T and incubated with a rabbit TeNT antiserum (Istituto Superiore di

Sanità, Rome, Italy) diluted in 1% BSA in PBS for 1 hour. After washing with PBST, wells were incubated with appropriate secondary antibody conjugated with HRP. Wells were extensively washed and 100 µL of 2,2'-azino-bis(3-ethylbenzothiazoline-6-sulfonic acid). Absorbance was read at 450 nm with a microplate reader (Tecan).

Low pH membrane translocation of TeNT in CGNs

CGNs were plated into 24-well plates at $4x10^5$ density and incubated in ice-cooled complete BME with either 10 nM TeNT or 10 nM TeNT preincubated with 20 nM TT110-Fab. This assay was then performed as described in (51) and the activity of the TeNT L domain into the cytosol was evaluated by western blotting following its VAMP-2 specific proteolytic activity as described above.

Fluorescence assay of ANS binding to clostridial neurotoxins as a function of pH

TeNT alone or TeNT preincubated with tenfold TT110-Fab were diluted to the final concentration of 0.8 µM in 100 mM TRIS-citrate buffer, 100 mM NaCl, pH 7.0 in the presence of liposomes (final concentration of 0.4 mM) and 50 µM ANS. The assay was then performed as previously described (56).

Mouse bioassay

Swiss-Webster adult CD1 mice (Charles River) were housed under controlled light/dark conditions, and food and water were provided ad libitum.

In pre-incubation assays, TeNT was diluted at a concentration of 8 pg/µl in bioassay solution, split into aliquots and supplemented either with an equivolume of bioassay solution (positive control) or an equivolume of bioassay solution supplemented with the indicated amounts of humAbs or Fabs under a gentle agitation for 1 hour at RT. Female mice (24–26 grams) were randomly injected intra peritoneum with 1 µl per gram of body weight of either toxin alone or toxin-humAbs/Fabs solutions. The final TeNT dose was 4 ng/kg, roughly corresponding to a fivefold lethal dose of our toxin preparation.

For the prophylactic activity, TIG (Igantet, Istituto Grifols Poligono Levante S.A., Italy) or humAbs (TT104 and TT110 alone or their combination) were diluted in bioassay solution and intraperitoneally injected with the indicated dose. After 7 or 15 days, TeNT (4 ng/kg) was injected intraperitoneally and mice were monitored for 200 hours, when the experiment was terminated. A human endpoint was set as to when mice showed moderate tetanus symptoms (hunched back and

paralysis of rear limbs or disappearance of the righting reflex for 30 s), after which the animal was euthanized by cervical dislocation and considered positive for tetanus. TIG was used at a dose of 7 IU/kg, roughly corresponding to the canonic prophylactic injection of 500 IU in a human of 70 kg.

To test the post-exposure effect of Fabs, TeNT (4 ng/kg) was i.p. injected. At the indicated time points, either TT104-Fab in combination with TT110-Fab (1.2 µg/kg) or TIG (7 IU/kg) were i.p. injected and mice monitored up to 200 hours. TIG dose was chosen to correspond to the suggested treatment of 500 IU in human of 70 kg. Fab doses were calculated accordingly, estimating the concentration of TeNT-specific IgGs in the serum of hyper-immunized subject equal to 40 µg/ml as averaged from values reported in (57).

Data were plotted as Kaplan-Meier survival curves and statistic measured with the Log-rank test. Each curve is representative of at least 6 animals. At each experiment at least 3 mice were treated with TeNT alone. The curve for survival of TeNT alone in Figure 2D and Figure 7B, 7C, 7D and 7F derive from all the data plotted together.

Statistics

Statistical analyses were carried out with GraphPad Prism. Statistical significance in ELISA assays was calculated using a two-tailed unpaired t tests. The curves of survival were compared using the Mantel-Cox log-rank test. In any case, results were considered significant when the *P* value was lower than 0.05.

Study Approval

Our studies were carried out in strict accordance with the European Community Council Directive n˚ 2010/63/UE and approved by the local (University of Padova) and national ethic committees of the Italian Ministry of Health.

Data deposition

Atomic coordinates and density maps have been deposited for immediate release as PDB ID 7OH0 and EMD-12890 for the HC-TT104-Fab region and as PDB ID 7OH1 and EMD-12891 for the L-HN-TT110-Fab region.

Author Contribution

Conceptualization, C.M., A.L. and G.Z.; Investigation M.P., A.G., O.L., F.V., M.T. S.B, D.C., C. SF., E.K., L.O.; Data Curation, A.G. and G.Z., Resources, G.S., S.B., D.C., C. SF., E.K., L.O.; Supervision, C.M., A.L. and G.Z. Writing Original Draft, C.M., A.L. G.Z., G.S. and M.P.; Writing, Reviewing and Editing, all authors.

Acknowledgements

We are grateful to the European Synchrotron Radiation Facility in Grenoble (France) for provision of beam time on CM01. We thank Dr. Gordon A. Leonard for the support in data collection and Prof. Ornella Rossetto for critical reading of the manuscript.
We gratefully acknowledge the financial support of the University of Padova (M.P. and C.M.), of the project RIPANE (C.M.), the Wellcome Trust (107116/Z/15/Z) [G.S.] and the UK Dementia Research Institute (UKDRI-1005) [G.S.].

Declaration of interests

A.L., L.P., C.S. and D.C. are employees of VIR Biotechnology and may hold shares in Vir Biotechnology.

References

1. Cook TM, Protheroe RT, and Handel JM. Tetanus: a review of the literature. *Br J Anaesth.* 2001;87(3):477-87.

2. Yen LM, and Thwaites CL. Tetanus. *Lancet.* 2019;393(10181):1657-68.

3. Popoff MR. Tetanus in animals. *J Vet Diagn Invest.* 2020;32(2):184-91.

4. Rossetto O, and Montecucco C. Tables of Toxicity of Botulinum and Tetanus Neurotoxins. *Toxins (Basel).* 2019;11(12).

5. Megighian A, Pirazzini M, Fabris F, Rossetto O, and Montecucco C. Tetanus and Tetanus Neurotoxin: from peripheral uptake to central nervous tissue targets. *J Neurochem.* 2021; doi: 10.1111/jnc.15330

6. Montecucco C, and Schiavo G. Structure and function of tetanus and botulinum neurotoxins. *Q Rev Biophys.* 1995;28(4):423-72.

7. Chapeton-Montes D, Plourde L, Bouchier C, Ma L, Diancourt L, Criscuolo A, Popoff MR, and Brüggemann H. The population structure of Clostridium tetani deduced from its pan-genome. *Sci Rep.* 2019;9(1):11220.

8. Masuyer G, Conrad J, and Stenmark P. The structure of the tetanus toxin reveals pH-mediated domain dynamics. *EMBO Rep.* 2017;18(8):1306-17.

9. Bruggemann H, Brzuszkiewicz E, Chapeton-Montes D, Plourde L, Speck D, and Popoff MR. Genomics of Clostridium tetani. *Res Microbiol.* 2015;166(4):326-31.

10. Schiavo G, Papini E, Genna G, and Montecucco C. An intact interchain disulfide bond is required for the neurotoxicity of tetanus toxin. *Infect Immun.* 1990;58(12):4136-41.

11. Rummel A, Bade S, Alves J, Bigalke H, and Binz T. Two carbohydrate binding sites in the H(CC)-domain of tetanus neurotoxin are required for toxicity. *J Mol Biol.* 2003;326(3):835-47.

12. Chen C, Baldwin MR, and Barbieri JT. Molecular basis for tetanus toxin coreceptor interactions. *Biochemistry.* 2008;47(27):7179-86.

13. Chen C, Fu Z, Kim JJ, Barbieri JT, and Baldwin MR. Gangliosides as high affinity receptors for tetanus neurotoxin. *J Biol Chem.* 2009;284(39):26569-77.

14. Bercsenyi K, Schmieg N, Bryson JB, Wallace M, Caccin P, Golding M, Zanotti G, Greensmith L, Nischt R, and Schiavo G. Nidogens are therapeutic targets for the prevention of tetanus. *Science.* 2014;346(6213):1118-23.

15. Deppe J, Weisemann J, Mahrhold S, and Rummel A. The 25 kDa HCN Domain of Clostridial Neurotoxins Is Indispensable for Their Neurotoxicity. *Toxins.* 2020;12(12).

16. Schiavo G, Matteoli M, and Montecucco C. Neurotoxins affecting neuroexocytosis. *Physiol Rev.* 2000;80(2):717-66.

17. Binz T, and Rummel A. Cell entry strategy of clostridial neurotoxins. *J Neurochem.* 2009;109(6):1584-95.

18. Deinhardt K, Berninghausen O, Willison HJ, Hopkins CR, and Schiavo G. Tetanus toxin is internalized by a sequential clathrin-dependent mechanism initiated within lipid microdomains and independent of epsin1. *J Cell Biol.* 2006;174(3):459-71.

19. Salinas S, Bilsland LG, Henaff D, Weston AE, Keriel A, Schiavo G, and Kremer EJ. CAR-associated vesicular transport of an adenovirus in motor neuron axons. *PLoS Pathog.* 2009;5(5):e1000442-e.

20. Schwab ME, and Thoenen H. Electron microscopic evidence for a transsynaptic migration of tetanus toxin in spinal cord motoneurons: An autoradiographic and morphometric study. *Brain Res.* 1976;105(2):213-27.

21. Matteoli M, Verderio C, Rossetto O, Iezzi N, Coco S, Schiavo G, and Montecucco C. Synaptic vesicle endocytosis mediates the entry of tetanus neurotoxin into hippocampal neurons. *Proc Natl Acad Sci U S A.* 1996;93(23):13310-5.

22. Pirazzini M, Bordin F, Rossetto O, Shone CC, Binz T, and Montecucco C. The thioredoxin reductase-thioredoxin system is involved in the entry of tetanus and botulinum neurotoxins in the cytosol of nerve terminals. *FEBS Lett.* 2013;587(2):150-5.

627 23. Schiavo G, Benfenati F, Poulain B, Rossetto O, Polverino de Laureto P, DasGupta BR, and
628 Montecucco C. Tetanus and botulinum-B neurotoxins block neurotransmitter release by
629 proteolytic cleavage of synaptobrevin. *Nature.* 1992;359(6398):832-5.

630 24. Jahn R, and Scheller RH. SNAREs--engines for membrane fusion. *Nat Rev Mol Cell Biol.*
631 2006;7(9):631-43.

632 25. Brooks VB, Curtis DR, and Eccles JC. The action of tetanus toxin on the inhibition of
633 motoneurones. *J Physiol.* 1957;135(3):655-72.

634 26. Brooks VB, Curtis DR, and Eccles JC. Mode of action of tetanus toxin. *Nature.*
635 1955;175(4446):120-1.

636 27. Amanna IJ, Carlson NE, and Slifka MK. Duration of humoral immunity to common viral and
637 vaccine antigens. *N Engl J Med.* 2007;357(19):1903-15.

638 28. Thwaites CL, Beeching NJ, and Newton CR. Maternal and neonatal tetanus. *Lancet.*
639 2015;385(9965):362-70.

640 29. Thwaites CL, and Loan HT. Eradication of tetanus. *Br Med Bull.* 2015;116(1):69-77.

641 30. Miranda-Filho Dde B, Ximenes RA, Barone AA, Vaz VL, Vieira AG, and Albuquerque VM.
642 Randomised controlled trial of tetanus treatment with antitetanus immunoglobulin by the
643 intrathecal or intramuscular route. *Bmj.* 2004;328(7440):615.

644 31. Kabura L, Ilibagiza D, Menten J, and Van den Ende J. Intrathecal vs. intramuscular
645 administration of human antitetanus immunoglobulin or equine tetanus antitoxin in the
646 treatment of tetanus: a meta-analysis. *Trop Med Int Health.* 2006;11(7):1075-81.

647 32. Nelson AL, Dhimolea E, and Reichert JM. Development trends for human monoclonal
648 antibody therapeutics. *Nat Rev Drug Discov.* 2010;9(10):767-74.

649 33. Traggiai E, Becker S, Subbarao K, Kolesnikova L, Uematsu Y, Gismondo MR, Murphy BR,
650 Rappuoli R, and Lanzavecchia A. An efficient method to make human monoclonal antibodies
651 from memory B cells: potent neutralization of SARS coronavirus. *Nat Med.* 2004;10(8):871-
652 5.

653 34. Lanzavecchia A, Corti D, and Sallusto F. Human monoclonal antibodies by immortalization of
654 memory B cells. *Curr Opin Biotechnol.* 2007;18(6):523-8.

655 35. Corti D, Voss J, Gamblin SJ, Codoni G, Macagno A, Jarrossay D, Vachieri SG, Pinna D, Minola
656 A, Vanzetta F, et al. A neutralizing antibody selected from plasma cells that binds to group 1
657 and group 2 influenza A hemagglutinins. *Science.* 2011;333(6044):850-6.

658 36. Corti D, Misasi J, Mulangu S, Stanley DA, Kanekiyo M, Wollen S, Ploquin A, Doria-Rose NA,
659 Staupe RP, Bailey M, et al. Protective monotherapy against lethal Ebola virus infection by a
660 potently neutralizing antibody. *Science.* 2016;351(6279):1339-42.

37. Pieper K, Tan J, Piccoli L, Foglierini M, Barbieri S, Chen Y, Silacci-Fregni C, Wolf T, Jarrossay D, Anderle M, et al. Public antibodies to malaria antigens generated by two LAIR1 insertion modalities. *Nature.* 2017;548(7669):597-601.

38. Tan J, Sack BK, Oyen D, Zenklusen I, Piccoli L, Barbieri S, Foglierini M, Fregni CS, Marcandalli J, Jongo S, et al. A public antibody lineage that potently inhibits malaria infection through dual binding to the circumsporozoite protein. *Nat Med.* 2018;24(4):401-7.

39. Aliprandini E, Takata DY, Lepique A, Kalil J, Boscardin SB, and Moro AM. An oligoclonal combination of human monoclonal antibodies able to neutralize tetanus toxin in vivo. *Toxicon X.* 2019;2:100006.

40. Zhang CM, Imoto Y, Hikima T, and Inoue T. Structural flexibility of the tetanus neurotoxin revealed by crystallographic and solution scattering analyses. *J Struct Biol X.* 2021;5:100045.

41. Zhang G, Yu R, Chi X, Chen Z, Hao M, Du P, Fan P, Liu Y, Dong Y, Fang T, et al. Tetanus vaccine-induced human neutralizing antibodies provide full protection against neurotoxin challenge in mice. *Int Immunopharmacol.* 2021;91:107297.

42. Wang Y, Wu C, Yu J, Lin S, Liu T, Zan L, Li N, Hong P, Wang X, Jia Z, et al. Structural basis of tetanus toxin neutralization by native human monoclonal antibodies. *Cell Rep.* 2021;35(5):109070.

43. Dong M, Masuyer G, and Stenmark P. Botulinum and Tetanus Neurotoxins. *Annu Rev Biochem.* 2018.

44. Azarnia Tehran D, and Pirazzini M. Preparation of Cerebellum Granule Neurons from Mouse or Rat Pups and Evaluation of Clostridial Neurotoxin Activity and Their Inhibitors by Western Blot and Immunohistochemistry. *Bio-protocol.* 2018;8(13):e2918.

45. Umland TC, Wingert LM, Swaminathan S, Furey WF, Schmidt JJ, and Sax M. Structure of the receptor binding fragment HC of tetanus neurotoxin. *Nat Struct Biol.* 1997;4(10):788-92.

46. Fotinou C, Emsley P, Black I, Ando H, Ishida H, Kiso M, Sinha KA, Fairweather NF, and Isaacs NW. The crystal structure of tetanus toxin Hc fragment complexed with a synthetic GT1b analogue suggests cross-linking between ganglioside receptors and the toxin. *J Biol Chem.* 2001;276(34):32274-81.

47. Jayaraman S, Eswaramoorthy S, Kumaran D, and Swaminathan S. Common binding site for disialyllactose and tri-peptide in C-fragment of tetanus neurotoxin. *Proteins.* 2005;61(2):288-95.

48. Krissinel E, and Henrick K. Inference of Macromolecular Assemblies from Crystalline State. *J Mol Biol.* 2007;372(3):774-97.

49. Lam KH, Guo Z, Krez N, Matsui T, Perry K, Weisemann J, Rummel A, Bowen ME, and Jin R. A viral-fusion-peptide-like molecular switch drives membrane insertion of botulinum neurotoxin A1. *Nat Commun.* 2018;9(1):5367.

50. Pirazzini M, Azarnia Tehran D, Leka O, Zanetti G, Rossetto O, and Montecucco C. On the translocation of botulinum and tetanus neurotoxins across the membrane of acidic intracellular compartments. *Biochim Biophys Acta.* 2016;1858(3):467-74.

51. Pirazzini M, Rossetto O, Bolognese P, Shone CC, and Montecucco C. Double anchorage to the membrane and intact inter-chain disulfide bond are required for the low pH induced entry of tetanus and botulinum neurotoxins into neurons. *Cell Microbiol.* 2011;13(11):1731-43.

52. Pirazzini M, Rossetto O, Bertasio C, Bordin F, Shone CC, Binz T, and Montecucco C. Time course and temperature dependence of the membrane translocation of tetanus and botulinum neurotoxins C and D in neurons. *Biochem Biophys Res Commun.* 2013;430(1):38-42.

53. Sun S, Suresh S, Liu H, Tepp WH, Johnson EA, Edwardson JM, and Chapman ER. Receptor binding enables botulinum neurotoxin B to sense low pH for translocation channel assembly. *Cell Host Microbe.* 2011;10(3):237-47.

54. Gambale F, and Montal M. Characterization of the channel properties of tetanus toxin in planar lipid bilayers. *Biophys J.* 1988;53(5):771-83.

55. Montecucco C, Schiavo G, Brunner J, Duflot E, Boquet P, and Roa M. Tetanus toxin is labeled with photoactivatable phospholipids at low pH. *Biochemistry.* 1986;25(4):919-24.

56. Puhar A, Johnson EA, Rossetto O, and Montecucco C. Comparison of the pH-induced conformational change of different clostridial neurotoxins. *Biochem Biophys Res Commun.* 2004;319(1):66-71.

57. Carrel S, Morell A, Skvaril F, and Barandun S. Human tetanus antibodies: Isolation and characterization with special reference to the IgG subclasses. *FEBS Lett.* 1972;19(4):305-7.

58. Vieira P, and Rajewsky K. The half-lives of serum immunoglobulins in adult mice. *Eur J Immunol.* 1988;18(2):313-6.

59. Mankarious S, Lee M, Fischer S, Pyun KH, Ochs HD, Oxelius VA, and Wedgwood RJ. The half-lives of IgG subclasses and specific antibodies in patients with primary immunodeficiency who are receiving intravenously administered immunoglobulin. *J Lab Clin Med.* 1988;112(5):634-40.

60. Hinton PR, Johlfs MG, Xiong JM, Hanestad K, Ong KC, Bullock C, Keller S, Tang MT, Tso JY, Vásquez M, et al. Engineered Human IgG Antibodies with Longer Serum Half-lives in Primates. *J Biol Chem.* 2004;279(8):6213-6.

61. Wang H, Yu R, Fang T, Yu T, Chi X, Zhang X, Liu S, Fu L, Yu C, and Chen W. Tetanus Neurotoxin Neutralizing Antibodies Screened from a Human Immune scFv Antibody Phage Display Library. *Toxins.* 2016;8(9):266.

62. Ghotloo S, Amiri MM, Khoshnoodi J, Abbasi E, Jeddi-Tehrani M, Golsaz-Shirazi F, and Shokri F. Contribution of Fc fragment of monoclonal antibodies to tetanus toxin neutralization. *Neurotox Res.* 2020;37(3):578-86.

734 63. Deinhardt K, Salinas S, Verastegui C, Watson R, Worth D, Hanrahan S, Bucci C, and Schiavo
735 G. Rab5 and Rab7 control endocytic sorting along the axonal retrograde transport pathway.
736 *Neuron.* 2006;52(2):293-305.

737 64. Naydenova K, and Russo CJ. Measuring the effects of particle orientation to improve the
738 efficiency of electron cryomicroscopy. *Nat Commun.* 2017;8(1):629.

739 65. Zheng SQ, Palovcak E, Armache JP, Verba KA, Cheng Y, and Agard DA. MotionCor2:
740 anisotropic correction of beam-induced motion for improved cryo-electron microscopy. *Nat*
741 *Methods.* 2017;14(4):331-2.

742 66. Zhang K. Gctf: Real-time CTF determination and correction. *J Struct Biol.* 2016;193(1):1-12.

743 67. Zivanov J, Nakane T, Forsberg BO, Kimanius D, Hagen WJ, Lindahl E, and Scheres SH. New
744 tools for automated high-resolution cryo-EM structure determination in RELION-3. *Elife.*
745 2018;7:e42166

746 68. Tang G, Peng L, Baldwin PR, Mann DS, Jiang W, Rees I, and Ludtke SJ. EMAN2: an extensible
747 image processing suite for electron microscopy. *J Struct Biol.* 2007;157(1):38-46.

748 69. Nakane T, Kimanius D, Lindahl E, and Scheres SH. Characterisation of molecular motions in
749 cryo-EM single-particle data by multi-body refinement in RELION. *Elife.* 2018;7:e36861

750 70. Ilca SL, Kotecha A, Sun X, Poranen MM, Stuart DI, and Huiskonen JT. Localized reconstruction
751 of subunits from electron cryomicroscopy images of macromolecular complexes. *Nat*
752 *Commun.* 2015;6(8843.

753 71. Zhou Q, Zhou N, and Wang HW. Particle segmentation algorithm for flexible single particle
754 reconstruction. *Biophys Rep.* 2017;3(1):43-55.

755

Figures and legends

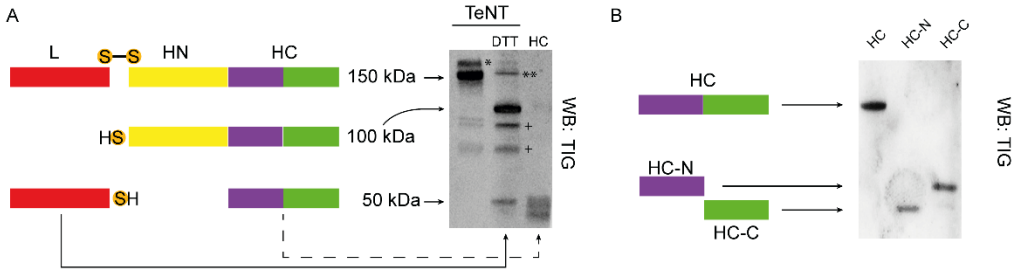

C

Antibody	TeNT	Reduced TeNT		Recombinant HC	Domain specificity
		L chain	H chain		
human antiserum	+	+	+	+	whole toxin
TT 4	+		+	+	HC
TT 13	+		+	+	HC
TT 16	+		+	+	HC
TT 33	+		+		HN
TT 39	+		+	+	HC
TT 102	+		+	+	HC
TT 103	+		+	+	HC
TT 104	+		+	+	HC
TT 107	+		+	+	HC
TT 108	+		+	+	HC
TT 109	+		+	+	HC
TT 110	+		+		HN
TT 114	+		+	+	HC
TT 115	+		+		HN

D

Antibody	Recombinant HC	Recombinant HC-N	Recombinant HC-C	Sub - domain specificity
human antiserum	+	+	+	whole HC
TT 4	+	+		HC-N
TT 13	+		+	HC-C
TT 16	+	+		HC-N
TT 39	+	+		HC-N
TT 102	+		+	HC-C
TT 103	+	+		HC-N
TT 104	+		+	HC-C
TT 107	+	+		HC-N
TT 108	+	+		HC-N
TT 109	+	+		HC-N
TT 114	+	+		HC-N

Figure 1. TeNT polypeptide chains and domain-specific recognition by TT-humAbs. A) Schematic structure of TeNT (top), TeNT-HC (middle). At the bottom the L chain (red) and HC subdomains HC-N (violet) and HC-C (green) and as they appear in western blotting (right panel) using TIG as primary antibody. Whole TeNT has a molecular weight of 150 kDa corresponding to the L chain + H chain (left line). Reduction with dithiothreitol (DTT) generates two bands corresponding to HC (HN+HC, 100 kDa) and L (50 kDa). Recombinant HC has a molecular weight of ~50 kDa. The L chain has weak signal possibly due to a low immunoreactivity of L-specific IgGs in TIG. *indicates a redox isomer of TeNT; **indicates single-chain TeNT; $^{+}$indicates degradation fragments. B) Schematic structure of HC (top), HC-N (middle) and HC-C (bottom) and how they appear in western blotting stained with TIG. C-D) Summary tables of TeNT domains and subdomains recognition by TT-humAbs as detected by western blotting. The specificity of TT-humAbs was determined with at least three independent trial per antibody.

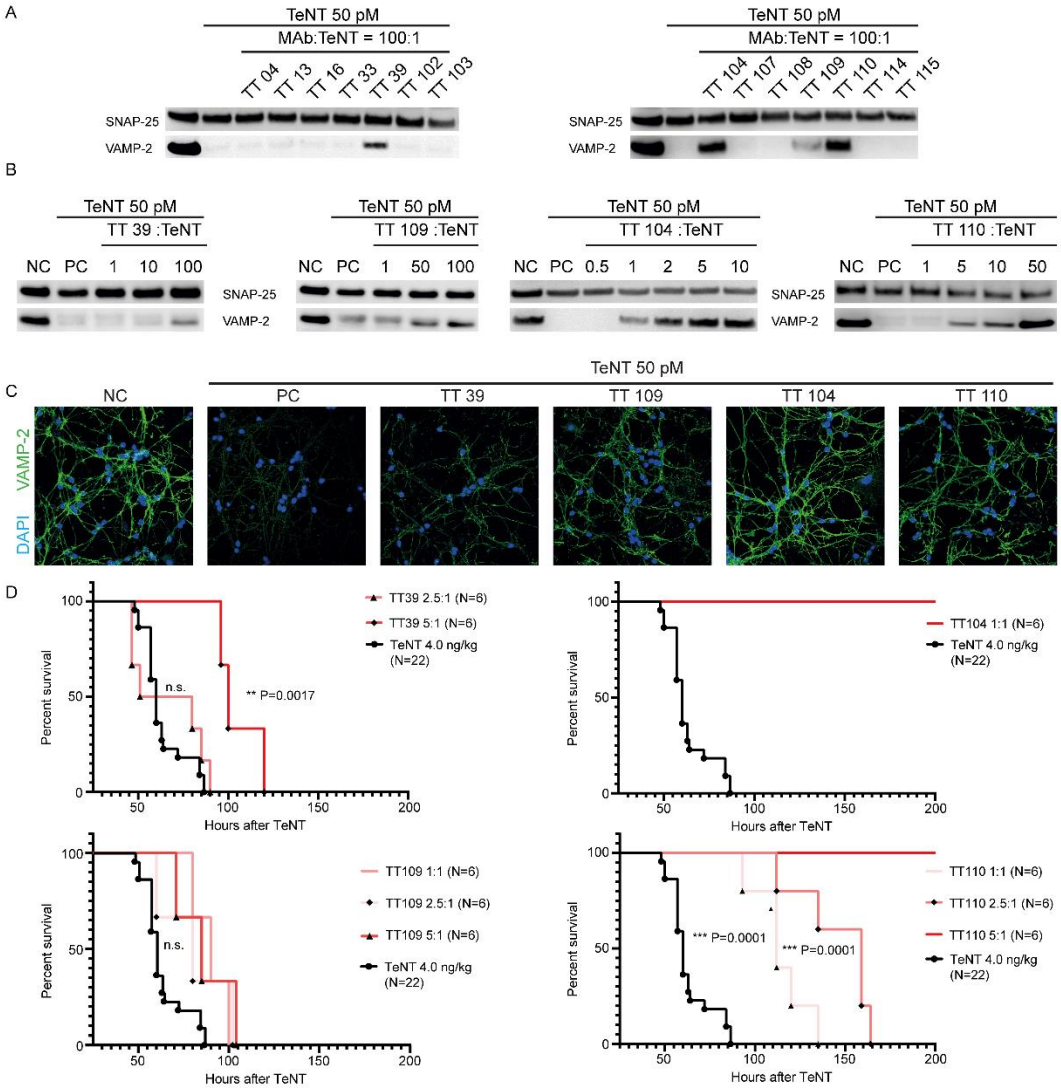

Figure 2. Preliminary screening for TeNT neutralization by TT-humAbs assayed *in vitro* and *in vivo*. A) TeNT (50 pM) was diluted in complete culture medium alone (PC) or supplemented with a 100X molar excess of the indicated humAb. The mixture was then added to CGNs for 12 hours and TeNT activity evaluated by monitoring the cleavage of VAMP-2 with an antibody recognizes only the intact form. SNAP-25 was used as loading control. NC indicates control CGNs. B) Effect of different TeNT:humAbs ratios for the humAbs displaying toxin neutralizing activity on CGNs. C) Immunofluorescence analysis performed with an antibody specific for intact VAMP-2 (green) to assay for the TeNT neutralizing activity of TT39, TT104, TT109 and TT110 preincubated with TeNT (100:1 molar ratio) and added to the primary culture of CGNs. Control CGNs (NC) are labelled in green whereas neurons treated with TeNT alone (PC) do not display this signal due to the complete cleavage of VAMP-2. CGNs treated with the indicated humAbs display intermediate signals depending on the neutralization activity of humAbs. Images are representative of three independent experiments. D) Mice were injected intraperitoneally with TeNT (4 ng/kg, black trace) alone or pre-incubated with the indicated molar ratios humAb:TeNT and survival plotted as a function of time after toxin injection. Statistical significance was calculated with Mantel-Cox test. Group numerosity is indicated in the panels.

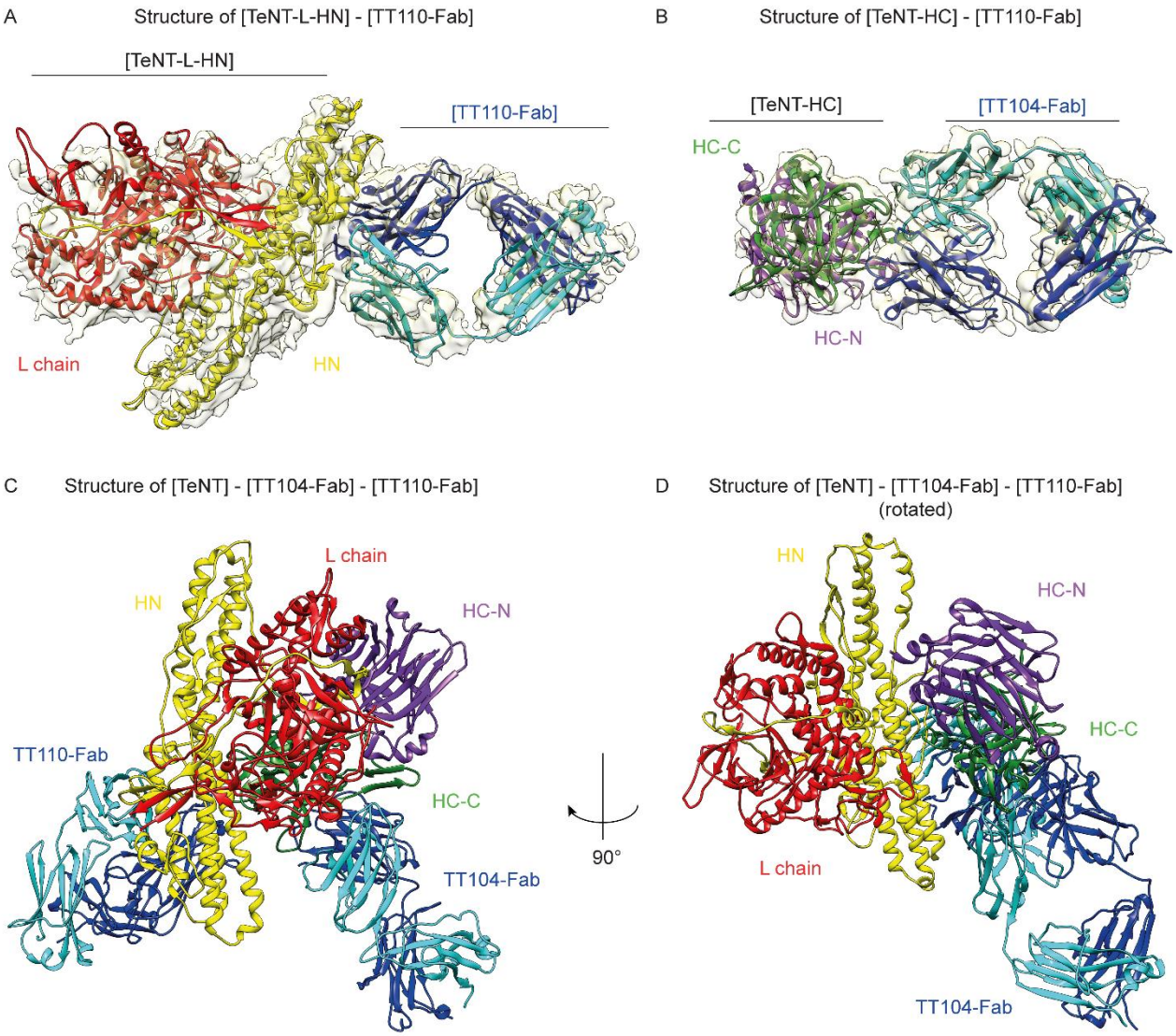

Figure 3. Cryo-EM structure of [TeNT-HC]-[TT104-Fab]-[TT110-Fab] ternary complex. A) Structure of HN (yellow) and L (red) domains in complex with TT110-Fab (light and dark blue for the variable L and H chain, respectively). B) Structure of the HC-C (green) and HC-N (purple) domains in complex with TT104-Fab (light and dark blue for the variable L and H chain, respectively). C-D) Overall structure of the TeNT-Fabs complex colored as in A and B.

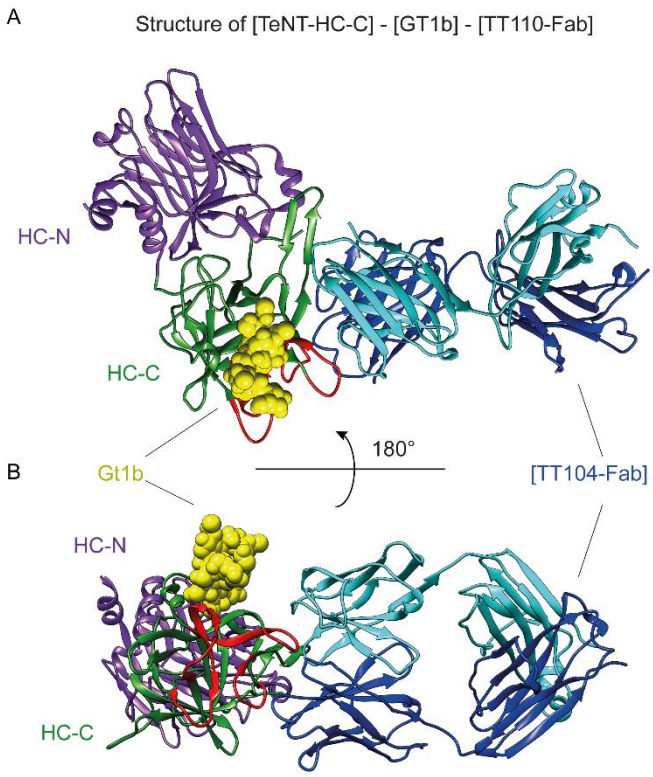

796

797 **Figure 4. Model of the [TeNT-HC]-[TT104-Fab] interaction in complex with GT1b.** A) The HC-N
798 (purple) and HC-C (green) domains of TeNT complexed with TT104-Fab (light and dark blue), and
799 the oligosaccharide portion of the GT1b colored in yellow (bound as in pdb:1FV3). In red is
800 highlighted the nidogen binding region. B) View of the model after a 180° horizontal rotation.
801

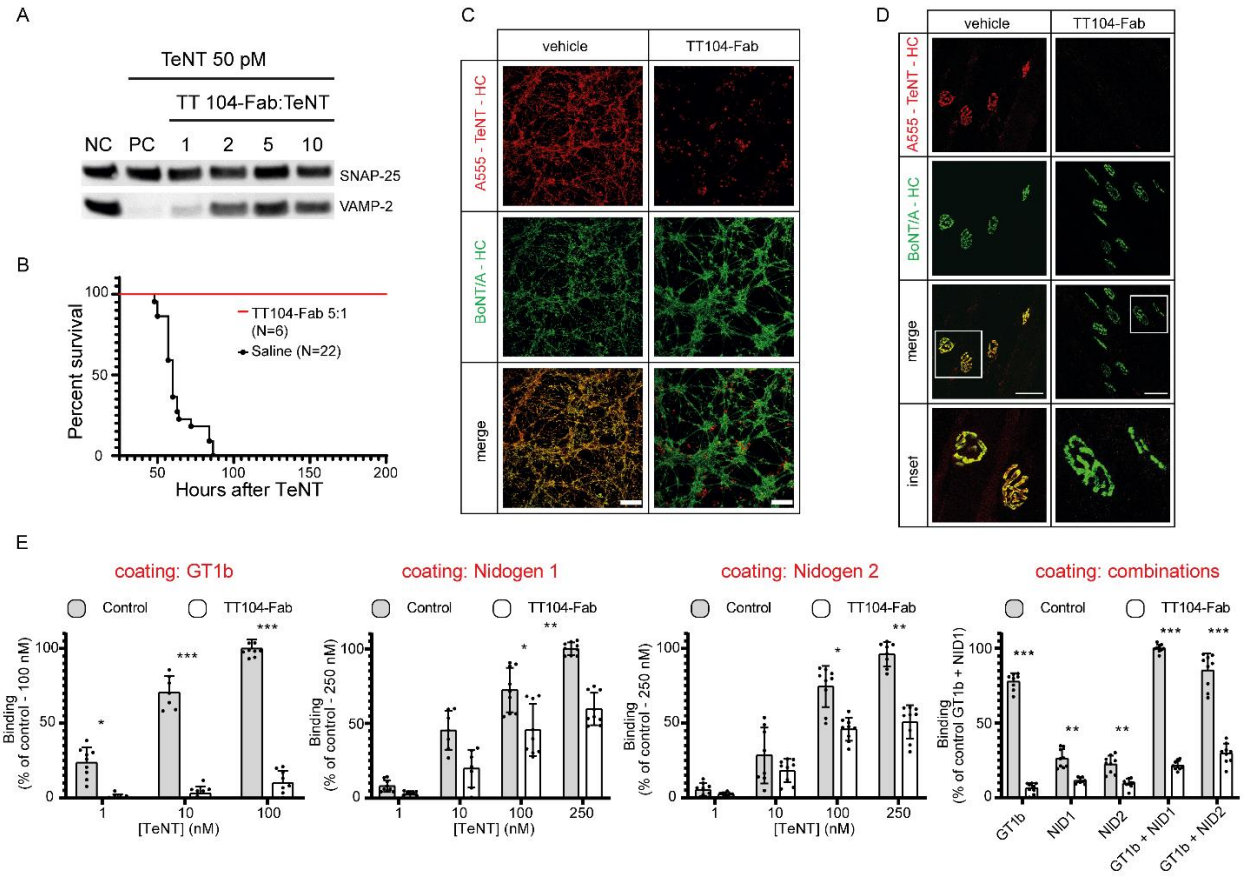

Figure 5. TT104-Fab prevents TeNT toxicity by interfering with toxin binding to polysialogangliosides and nidogen. A) Western blotting analysis of CGNs treated with 50 pM TeNT alone (PC) or preincubated with the indicated TT104-Fab:TeNT molar ratios. After 12 hours, TeNT activity was evaluated by monitoring the cleavage of VAMP-2 as in Figure 2. NC indicates control CGNs. Shown is one representative out of three independent experiments. B) Survival of mice injected intraperitoneally either with TeNT alone (4 ng/kg) or premixed with 5:1 molar ratio TT104-Fab:TeNT. Group numerosity is indicated within the panel. C) Fluorescence in CGNs treated with a mixture of 50 nM A555-TeNT-HC (red) or 50 nM CpV-BoNT/A-HC (green) preincubated either with culture medium or with a 2:1 molar ratio of TT104-Fab:TeNT-HC for 2 hours and observed with a confocal microscope. Images are representative of one representative out of three independent experiments. D) Immunofluorescence staining of the *Levatoris Aureus Longus* muscle injected *in vivo* with A555-TeNT-HC (1 µg) or CpV-BoNT/A-HC (1 µg) preincubated either with vehicle or with a 2:1 molar ratio of TT104-Fab:TeNT and observed after 2 hours with a confocal microscope. Images are representative of one representative out of three independent experiments. E) Purified GT1b (0.5 µg/well, left panel), recombinant nidogen-1/2 (250 ng/well, middle right and middle left panels) or their combination (right panel) were adsorbed by overnight incubation on ELISA plates and the binding of indicated concentrations of either TeNT alone (filled columns) or TeNT preincubated with TT110-Fab (white columns) was tested as described previously (12). Data are reported as percentage of the highest value in the graph and averaged from at least three independent experiments (each dot represent a single well). Graphs show mean±S.D. Significance was calculated by a two tailed t test (*=P<0.05, **=P<0.01; ***P<0.001).

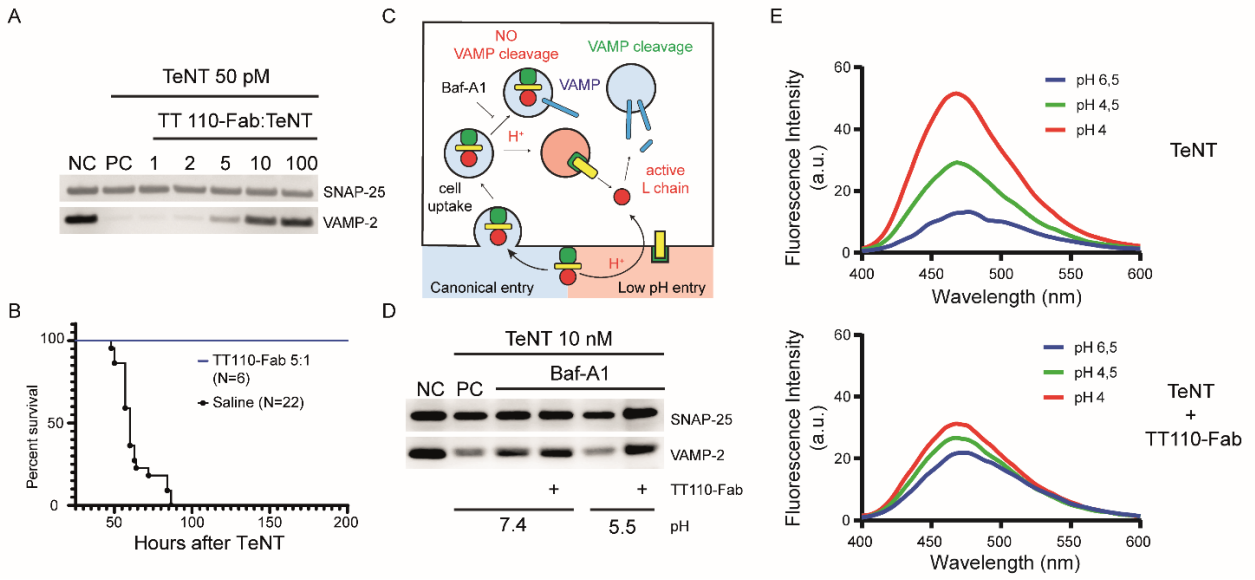

Figure 6. TT110-Fab neutralizes TeNT toxicity by preventing the translocation of the L chain into the nerve terminal cytosol. A) Western blotting of CGNs treated with 50 pM TeNT alone (PC) or preincubated with the indicated TT104-Fab:TeNT molar ratio. After 12 hours, CGNs were lysed and immunoblotted for VAMP-2 and SNAP-25 as in Figure 2. NC indicates control CGNs. Shown is one representative out of three independent experiments. B) Survival curve of mice injected intraperitoneally with either TeNT alone (4 ng/kg) or premixed with 5X molar excess of TT104-Fab. Group numerosity is indicated within the panel. C) Scheme illustrating the entry of TeNT L chain into the neuronal cytosol via either: the canonical receptor-mediated cell uptake and translocation across the membrane of synaptic vesicles triggered by the acidification of their lumen due to the proton pump activity of the V-ATPase (light blue) or the low-pH translocation across the plasma membrane in the presence of bafilomycin A1 (Baf-A1). D) Western blotting analysis showing the inhibition of TeNT L chain membrane translocation by TT110-Fab. CGNs were incubated at 4°C for 15 minutes with either TeNT (10 nM) or TeNT preincubated with TT110-Fab. The culture medium was then replaced with a 37°C buffer for 10 minutes either at pH 7.4 or pH 5.0. Samples were then incubated for 12 hours with normal medium (PC) or normal medium supplemented with Baf-A1 (100 nM). Membrane translocation was assessed by VAMP-2 cleavage. SNAP-25 served as loading control. NC indicates control CGNs. Shown is one representative out of three independent experiments. E) ANS fluorescence binding experiment showing the pH-induced conformational change of TeNT blocked by TT110-Fab. TeNT (0.35 µM) (top) or TeNT pre-incubated with TT110-Fab (bottom) were incubated at pH 7.0 in the presence of 50 µM ANS and liposomes. The conformational change was triggered by lowering the pH with sequential addition of specific volumes of HCl and evaluated following the ANS fluorescence intensity at 470 nm. Shown is one representative out of two independent experiments.

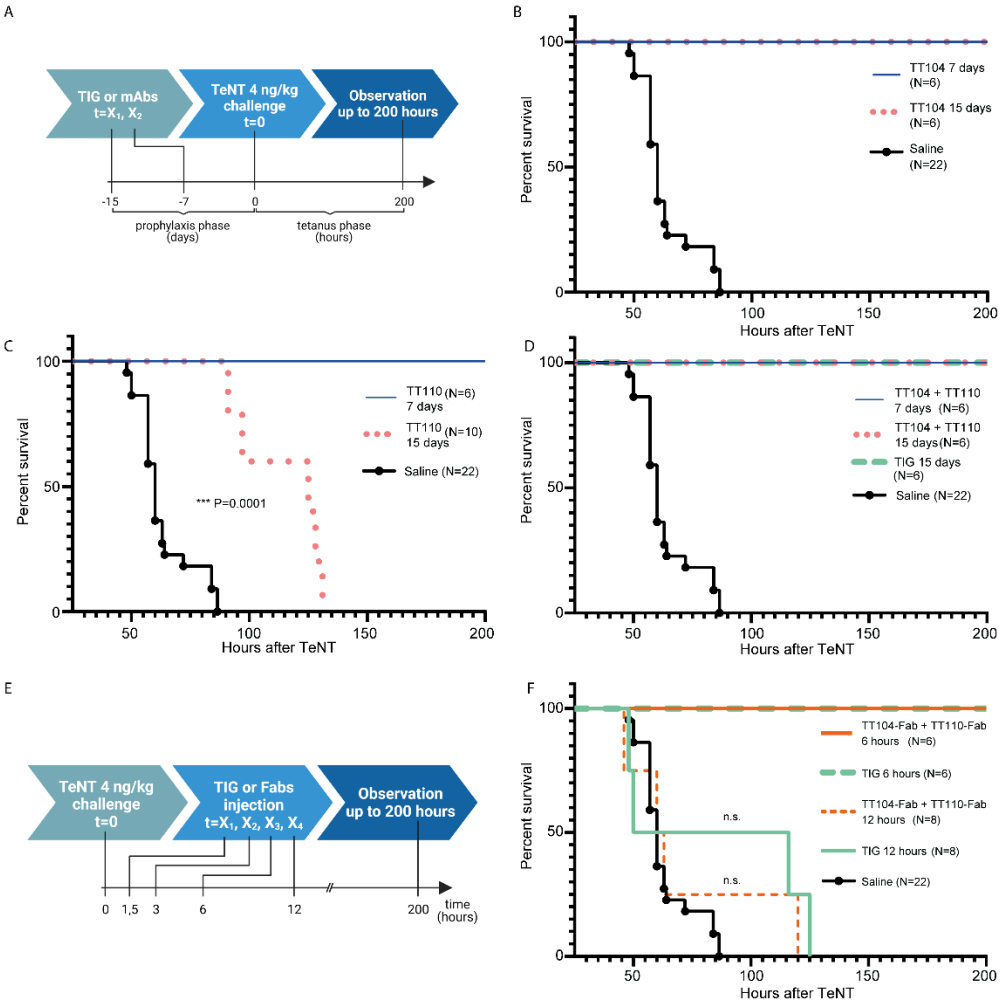

Figure 7. TT104 and TT110 HumAbs allow a long-lasting prophylactic protection against TeNT and their Fabs derivatives prevent tetanus development after toxin challenge. A) Time-course to test the prophylactic activity of humAbs. Mice were intraperitoneally pre-injected with either TT104 (400 ng/kg) or TT110 (400 ng/kg) or their combination (200 ng/kg+200 ng/kg) or with TIG (3.5 IU/kg roughly corresponding to 250 IU/70 kg) for 15 or 7 days. TeNT (4 ng/kg) was then inoculated intra-peritoneally and the animals observed for 200 hours for tetanus symptoms. The prophylactic profiles for TT104 and TT110 injected alone are shown in (B) and (C), respectively. Panel D shows the survival curves of TT104+TT110 in combination compared to TIG. E) Time-course to test TeNT neutralization by Fabs in post-exposure challenge. TeNT (4 ng/kg) was inoculated via intraperitoneal injection. At indicated times, the combination of TT104 + TT110 Fab derivatives (1.2 µg/kg) or TIG (7 IU/kg) were injected intra peritoneum and the animals observed for 200 hours. F) Survival plot of mice injected with TeNT and treated with either TT104 + TT110 Fab derivatives (1.2 µg/kg, orange traces) or TIG (7 IU/kg, cyan traces) after 6 or 12 hours. Statistical significance was calculated with Mantel-Cox test. Group numerosity is indicated within the panels. Panels 7B, 7C, 7D and 7F display the same lethality curve for the saline group as they derive from the data of all the mice treated with TeNT alone plotted together.

Table 1: TeNT neutralization *in vivo* showing the prophylactic and therapeutic activities of HumAbs and Fabs. HumAbs, TIG or Fab were injected at the indicated time points with respect to TeNT inoculation. Survival percentage was calculated based on animals surviving up to 200 hours.

Prophylactic use			
Agent	**Dose**	**Time before TeNT injection (days)**	**% survival**
HumAbs combination	400 ng/kg	7 days	100 %
		15 days	100 %
TIG	3.5 U/kg (corresponding to 0.6 µg/kg of specific anti-TeNT IgGs and to ~ 2.5 mg/kg of total proteins)	15 days	100 %
Therapeutic use			
Agent	**Dose**	**Time after TeNT injection (hours)**	**% survival**
Fab combination	1.2 µg/kg	1.5 h	100 %
		3 h	100 %
		6 h	100 %
TIG	7 U/kg (corresponding to 1.2 µg/kg of specific anti-TeNT IgGs and to ~ 5 mg/kg of total proteins)	1.5 h	100 %
		3 h	100 %
		6 h	100 %